N O T I C E

THIS DOCUMENT HAS BEEN REPRODUCED FROM
MICROFICHE. ALTHOUGH IT IS RECOGNIZED THAT
CERTAIN PORTIONS ARE ILLEGIBLE, IT IS BEING RELEASED
IN THE INTEREST OF MAKING AVAILABLE AS MUCH
INFORMATION AS POSSIBLE

Structural Dynamics of Shroudless, Hollow Fan Blades With Composite In-Lays

R. A. Aiello, M. S. Hirschbein, and C. C. Chamis
Lewis Research Center
Clevelund, Ohio

NASA

STRUCTURAL DYNAMICS OF SHROUDLESS, HOLLOW FAN BLADES

WITH COMPOSITE IN-LAYS

by

R. A. Aiello, M. S. Hirschbein, and C. C. Chamis
National Aeronautics and Space Administration
Lewis Research Center
Cleveland, Ohio, U.S.A.

ABSTRACT

Structural and dynamic analyses are presented for a shroudless, hollow titanium fan blade proposed for future use in aircraft turbine engines. The blade was modeled and analyzed using the Lewis Research Center's Composite Blade Structural Analysis Computer Program (COBSTRAN). COBSTRAN is an integrated program consisting of mesh generators, composite mechanics codes, NASTRAN, and pre- and post-processors. Vibration and impact analyses are presented. The vibration analysis was conducted with COBSTRAN. Results show the effect of the centrifugal force field on frequencies, twist, and blade camber. Bird impact analysis was performed with the Multi-Mode Blade Impact Computer Program. This program uses the geometric model and modal analysis from the COBSTRAN vibration analysis to determine the gross impact response of the fan blades to bird strikes. The structural performance of this blade is also compared to a blade of similar design but with composite in-lays on the outer surface. Results show that the composite in-lays can be selected (designed) to substantially modify the mechanical performance of the shroudless, hollow fan blade.

INTRODUCTION

The shroudless, hollow titanium fan blade design incorporates advanced fabrication, aerodynamic and structural concepts. The improved fan efficiency resulting from this advanced design represents up to a 2 percent efficiency gain which is a significant portion of the total performance improvement goal (about 12 percent) for an energy efficient engine. Therefore, this analysis was made to evaluate the present design and to aid in determining the risks involved using this type of blade as well as to demonstrate improvements in structural performance by using composite in-lays.

ANALYSIS METHODS

NASA Lewis Research Center's Composite Blade Structural Analysis computer code (COBSTRAN) was used for the structural and dynamic analysis of the fan blades. This code models a blade composed of various layers of materials as a solid blade having the same structural properties as the layered blade. This form of modeling simplifies the analysis of blades with composite in-lays on the surface or internal voids. For the blade with composite in-lays the fiber direction is parallel to the span. The hollow blade was modeled such that the solid sections were layers of titanium and the hollow sections were simulated by layers of a soft, low

density artificial material. Compared to modeling the hollow part as a shell, this modeling approach: (1) predicts the same structural response; (2) has about 25 percent fewer elements; (3) uses plate bending elements throughout; (4) simplifies rib modeling; and (5) uses the mean camber line for element connections. Equivalent homogeneous section properties were calculated at each node from the nodal thickness and material properties. A finite element mesh of triangular elements and their properties was generated in a format compatible with NASTRAN input data requirements.

A modified form of the Interactive Multi-Mode Blade Impact (MMBI) computer code, developed under contract for NASA (ref. 2) was used to model a bird strike. This code models the bird as a composite of 2-D and 3-D fluid jets. The blade is modeled by a set of normal modes. During the impact event the program calculates the pressure loading on the face of the blade accounting for instantaneous blade position, including blade motion, and curvature of the blade chord. The blade response is then calculated incrementally using modal synthesis over each time step.

A computer code (ZULU) was written specifically to convert the blade profile data to a form compatible with the input requirements of COBSTRAN (ref. 1)

FINITE ELEMENT MODEL

The external profile and internal cavity details of the blade were obtained from a preliminary design. Blade stations selected for the analysis are from a radius of 15.3 in. (0.389 m) at the root of the blade to a radius of 43.2 in. (1.10 m) at the tip or a span of about 30 in. (0.762 m). The blade had an aspect ratio of 2.5, a hub-tip ratio of 0.34, a weighted average pressure ratio of 1.7 and a tip speed of about 1500 ft/sec (457 m/s) at design speed. The weight of the blade modeled by NASTRAN is 18.2 lb (8.27 kg).

The finite element model was generated by establishing node points along the mean camber line of each of 34 blade stations for a total of 433 nodes. These nodes were connected by 777 triangular plate bending elements. The thickness of each element was obtained by averaging the blade thickness at each of its nodes. A computer plot of the finite element model used for the NASTRAN analysis is shown in figure 1.

All constraint to blade motion was at the nine nodes of station 15.3 (blade root). Eight of the nodes were constrained in five degrees of freedom (DOF) but allowed to translate in the direction of the axis of rotation (chord-wise at the root). The middle node was constrained in all six degrees of freedom. The blade as modeled contains 2552 degrees of freedom which is considered to be more than adequate for this structural analysis.

ANALYSIS AND RESULTS

All-Titanium Blade

Vibration modes of the blade were calculated under a no-load condition and also at various rotational speeds to include the effect of centrifugal stiffening. The frequencies determined for the all-titanium hollow blade are summarized in table I. These results were obtained by using constraints along the blade root as described previously.

2

The frequencies in parentheses in table I were obtained by constraining the blade along the platform streamline in the same manner as for the blade root. Constraint along this streamline implies a rigid locking of the blade in the rotor. Therefore these results can be considered only as an upper bound of the frequency range.

The effects of centrifugal force stiffening on the frequencies are customarily presented as a plot of frequency vs. rotor speed (Campbell diagram) as shown in figure 2 in which are also shown the integral order resonances at the intersection with the engine order lines. The corresponding mode shapes are shown in figure 3.

The twist of the blade is reduced as the centrifugal force is increased. The reduction in blade twist along the span at 4000 rpm is shown in figure 4. The maximum change in twist is about 5 degrees at the tip. This reduction in twist (untwist) is substantial and, therefore, its effect on blade performance should be carefully evaluated. This is especially critical since the pressure ratio is very sensitive to small changes in the incidence angle.

The change in blade camber along the span at 4000 rpm is shown in figure 5. Camber angle decreases in the solid sections of the blade and increases in the hollow sections. The camber also decreases at the tip. The maximum change in camber is about a 0.6 degree increase midway through the hollow span of the blade. This change in camber is significant compared to acceptable standards for a shrouded blade.

An indicator of possible blade torsional flutter at minimum cruise, used in preliminary design, is the "reduced-velocity parameter" defined as:

$$V_r = \frac{w}{b\,f_t}$$

where

b = 1/2 chord at 5/6 span (ft)

w = average air velocity relative to the blade over the outer 1/3 of the span (ft/sec)

f_t = first torsional frequency at design rpm (rad/sec)

Experience has shown that, for this case, a value of V_r greater than about 1.4 indicates possible blade torsional flutter when operated at minimum cruise speed. The values of the three terms determined for this blade at aircraft cruise conditions are:

b = 0.56 ft, w = 1400 ft/sec, f_t = 1670 rad/sec
(0.171 m)   (427 m/s)

The calculated value of the "reduced-velocity parameter" is 1.5. Based on this parameter a possible flutter problem exists in the 3rd (first torsional) mode.

A comparison of the bird strike tolerance was modeled by considering the impact from a 1 lb (0.455 kg) fluid sphere with an impact speed of 900 ft/sec (274 m/s). The diameter of the simulated bird was 3.75 in. (9.73 cm). The impact point was near the 70 percent span position, and

3

the missile first contacted the blade about 2 in. (5.08 cm) back from the leading edge. The impact angle was 25 degrees relative to the chord line. The first 6 modes at 4000 rpm, obtained using COBSTRAN, were used to synthesize the blade response to impact using the MMBI code.

The radial stress in the all-titanium blade due to impact is shown in figure 6. The response is for a point near the stacking axis on the impacted side of the blade about 1 in. (2.54 cm) above the base of the blade. This region of the blade carries most of the steady and impact loading. The impact event lasted about 0.7 millisec. The peak stress is about 110,000 psi (758 MPa). The stress response at other points near the base show the same basic time history with the peak stress being slightly higher near the leading edge. The maximum steady root stress at the reference point is 41,000 psi (282 MPa). Based on a yield strength of 125,000 psi (861 MPa) for titanium, the current blade design apparently will yield under the combined stress of the bird strike and the steady state stress (151,000 vs. 125,000 psi) at the reference point.

It should be noted that the impact analysis considered in this paper is inherently limited to small deformation and is not intended for a detailed analysis of local or severe impact damage. However, it can be used to assess the gross loading near the blade root. The tolerance at the impact region, however, needs to be assessed by a detailed stress analysis which accounts for nonlinear geometry and material effects.

Titanium Blade with Composite In-Lays

A modified hollow titanium blade with an outer surface of inlaid boron/aluminum composite was considered as a possible improvement to the basic all-titanium blade. The modified blade has the same dimensions as the basic blade except that three layers of 0.007 in. (0.0178 cm) thick unidirectional boron/aluminum composite have replaced the outer 0.021 in. (0.0533 cm) of titanium. The primary effect of the composite in-lays is to stiffen and lighten the blade. A comparison of the general structural performance of both blades is shown in table II.

The most significant change is to the 3rd mode frequency (first torsion) which increased by 20 percent at 4000 rpm for the blade with composite in-lays. This correspondingly increased the reduced-velocity flutter parameter from a negative margin of 0.1 to a positive margin of 0.26. The amount of untwist showed a comparable decrease of 24 percent at 4000 rpm. The absolute value of the camber change at 4000 rpm was reduced by about one-half compared to the all-titanium blade. Also noteworthy are the increases in the frequency of the first mode of the blade with the in-lays. These increases will shift the first mode intersection with the second engine order (2E) line (figure 2) to about 2500 rpm which is well below the 80 percent operating speed (minimum cruise speed).

The impact response of the blade with composite in-lays is shown in figure 7. The impact conditions and reference point are the same as for the all-titanium blade. The stress shown in figure 7 is for the titanium part of the blade. It is seen that the maximum radial impact stress in the titanium is about 120,000 psi (827 MPa). This is slightly higher than for the all-titanium blade. The stress distribution in the boron/ aluminum composite has the same shape but almost twice the magnitude. As such, the modified blade is a well balanced hybrid since the failure stress of the composite is about twice the yield stress of the titanium.

4

The maximum steady radial stress showed the same behavior. This stress in the titanium is 40,000 psi (276 MPa) at the reference point, slightly less than for the all-titanium blade, and the maximum radial steady stress in the composite is 82,C00 psi (551 MPa). It is noted that the composite in-lays are diffusion-bonded to the titanium substrate. The diffusion bond provides substantial interlaminar shear resistance at the composite in-lay/titanium interface.

SUMMARY

The results of the structural dynamics analysis of shroudless, hollow, all-titanium fan blades and hollow titanium blades with composite in-lays are as follows:

1. The effect of engine speed on the untwist of both hollow titanium blades is substantial and should be carefully considered in the evaluation of blade performance since the aerodynamic load may couple and magnify this effect as well as influence the blade flutter stability.

2. The effect of engine speed on the camber of both hollow titanium blades is relatively significant compared to acceptable changes permitted for this parameter.

3. A possible blade flutter problem is indicated in the 3rd (first torsional) mode for the hollow all-titanium blade.

4. The impact tolerance to bird strikes more than likely will yield both hollow titanium blades.

5. The blade with the composite in-lays has a positive torsional flutter margin, substantially less twist and uncamber and about the same impact tolerance at the root as the all-titanium blade.

6. The design concept of shroudless, hollow titanium blades with composite in-lays appears to be an effective approach to design energy efficient fan blades for high bypass ratio turbofan engines.

REFERENCES

1. Chamis, C. C., "Integrated Analysis of Engine Structures", NASA TM 82713, 1981.

2. Alexander, A., Cornell, R., "Interactive Multi-Mode Blade Impact Analysis" NASA CR 159462, Aug. 1979.

TABLE I. - HOLLOW ALL-TITANIUM BLADE

FREQUENCY - CPS

rpm	Mode 1	Mode 2	Mode 3
0	48.2	142.1	252.1
1000	54.8	148.3	253.5
2000	70.5	165.0	257.3
3000	90.3	188.9	263.2
4000	111.8 (115.2)*	216.4 (229.2)	270.8 (280.8)

*The frequencies in parentheses were ob-
tained by constraining the blade along
the platform streamline.

TABLE II. - COMPARISON OF BLADE PERFORMANCE CHARACTERISTICS

	Hollow all-titanium	Hollow titanium with boron/aluminum in-lays	Percent change
Frequency (H_z)			
0 rpm mode 1	43.2	56.3	+17
2	142.1	167.8	+18
3	252.1	309.9	+23
4000 rpm mode 1	111.8	115.9	+4
2	216.4	234.4	+8
3	270.8	326.3	+20
Weight (lb)	18.2	17.1	-6
Untwist (4000 rpm)			
100 percent span	5.37 degrees	4.06 degrees	-24
70 percent span	3.53 degrees	2.88 degrees	-18
Camber change (4000 rpm)			
100 percent span	-.27 degrees	-.13 degrees	-52
70 percent span	+.62 degrees	+.34 degrees	-45
Flutter margin (relative to 1.4)	-.1	+.26	

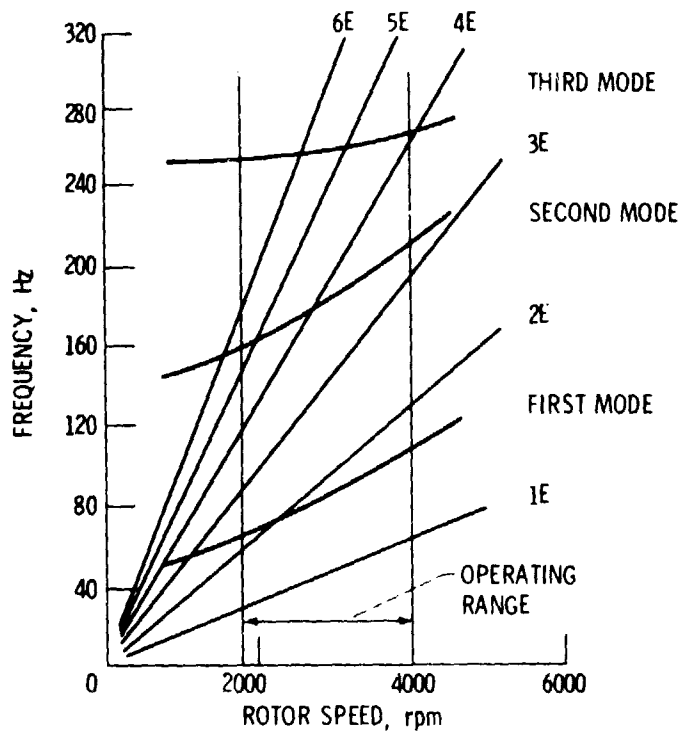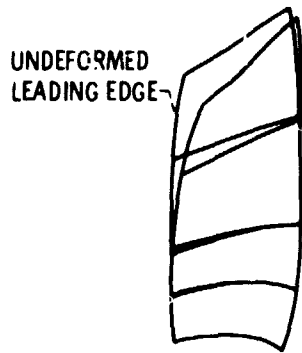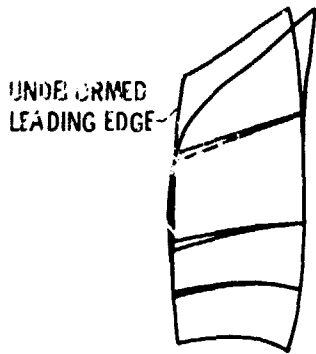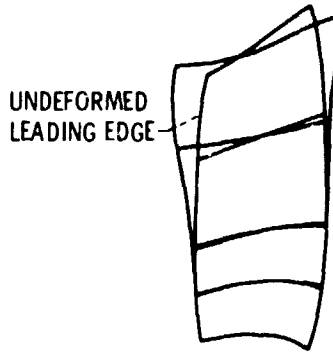Figure 1. - Nastran model of the hollow fan blade (777 elements).

Figure 2. - Campbell diagram for the all-titanium hollow fan blade.

UNDEFORMED
LEADING EDGE

(a) 1ST MODE SHAPE.
0 rpm FREQUENCY 48. 2 Hz
4000 rpm FREQUENCY 111.8 Hz

UNDEFORMED
LEADING EDGE

(b) 2ND MODE SHAPE.
0 rpm FREQUENCY 142.0 Hz
4000 rpm FREQUENCY 216.4 Hz

UNDEFORMED
LEADING EDGE

(c) 3RD MODE SHAPE.
0 rpm FREQUENCY 252.1 Hz
4000 rpm FREQUENCY 270.8 Hz

Figure 3. - Vibration mode shapes for the all-titanium hollow fan
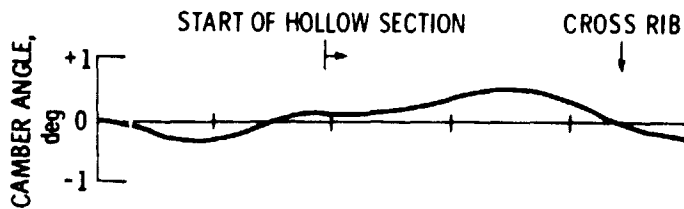blade (blade constrained at the root).

START OF HOLLOW SECTION   CROSS RIB

CAMBER ANGLE, deg

+1

0

-1

Figure 4. - Change in camber for the all-titanium fan
blade at 4000 rpm.

START OF HOLLOW SECTION   CROSS RIB
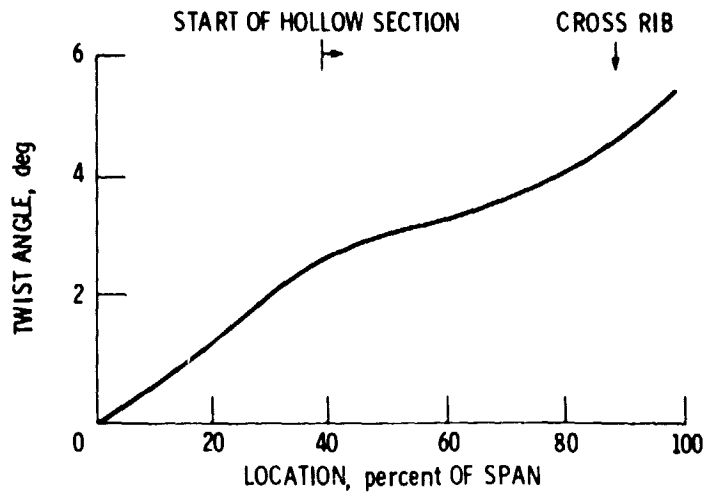
Figure 5. - Reduction in twist for the all-titanium fan
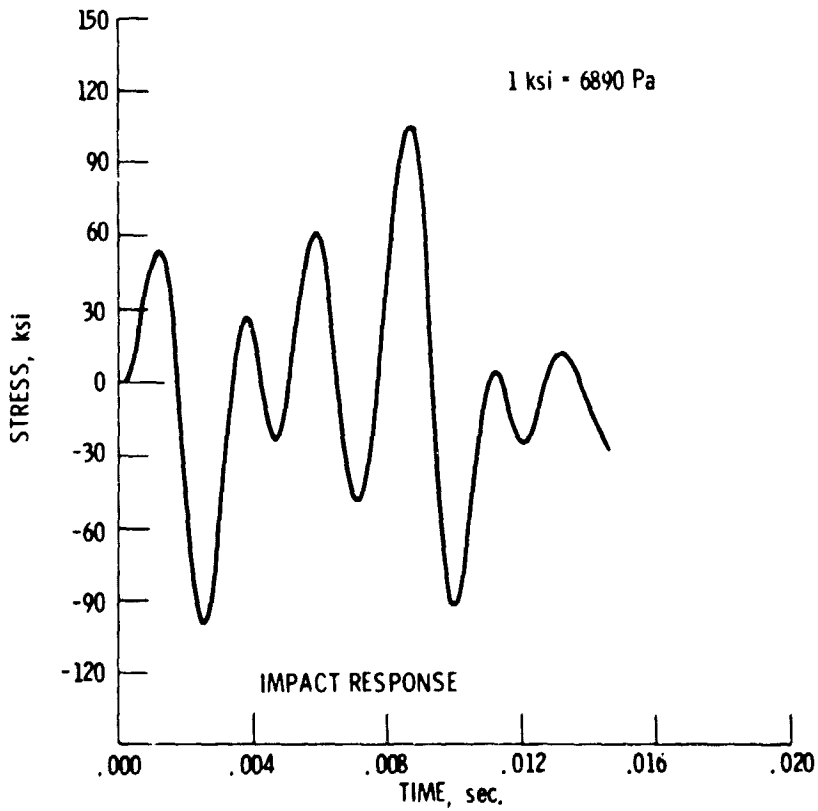blade at 4000 rpm.

1 ksi = 6890 Pa

IMPACT RESPONSE

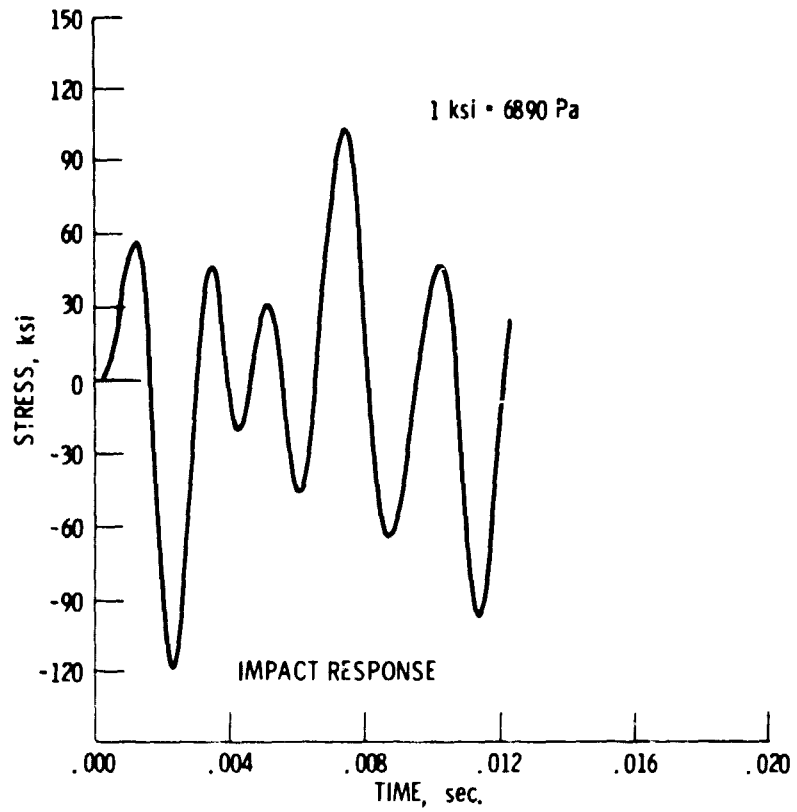Figure 6. - Radial stress in the all-titanium hollow fan blade.

Figure 7. - Radial stress in the titanium /composite hollow fan
blade.